Classification: BIOLOGICAL SCIENCES: Biochemistry

Overexpression in yeast, photocycle, and *in vitro* structural change of an avian putative magnetoreceptor Cryptochrome4

Hiromasa Mitsui[a], Toshinori Maeda[a], Chiaki Yamaguchi[a], Yusuke Tsuji[a], Ryuji Watari[a], Yoko Kubo[a], Keiko Okano[a], and Toshiyuki Okano[a, 1]

[a] Department of Electrical Engineering and Bioscience, Graduate School of Advanced Science and Engineering, Waseda University, Wakamatsu-cho 2-2, Shinjuku-ku, Tokyo 162-8480, Japan

Running title: Spectroscopic and biochemical analysis of cCRY4

To whom correspondence should be addressed: Dr. Toshiyuki Okano, Department of Electrical Engineering and Bioscience, Graduate School of Advanced Science and Engineering, Waseda University, Wakamatsu-cho 2-2, Shinjuku-ku, Tokyo 162-8480, Japan, Tel and Fax: +81-3-5369-7316
E-mail: okano@waseda.jp

Keywords: cryptochrome; recombinant protein expression; budding yeast; flavoprotein; photoreceptor; conformational change; spectroscopy; chromophore photoreduction; photocycle

ABSTRACT

Cryptochromes (CRYs) have been found in a wide variety of living organisms and can function as blue light photoreceptors, circadian clock molecules, or magnetoreceptors. Non-mammalian vertebrates have CRY4 in addition to the CRY1 and CRY2 circadian clock components. Though the function of CRY4 is not well understood, chicken CRY4 (cCRY4) may be a magnetoreceptor due to its high expression in the retina and light-dependent structural changes in retinal homogenates. In order to further characterize the photosensitive nature of cCRY4 at a molecular level, we developed a novel expression system using budding yeast and purified cCRY4 at yields of sub-milligram proteins per liter with binding of the flavin adenine dinucleotide (FAD) chromophore. Recombinant cCRY4 dissociated from anti-cCRY4 C1 mAb in a light-dependent manner and showed light-dependent change in its trypsin digestion pattern, strongly suggesting that cCRY4 changes its conformation with light irradiation in the absence of other retinal factors. Combinatorial analyses with UV-visible spectroscopy and immunoprecipitation revealed that there is chromophore reduction in the cCRY4 photocycle and formation of a flavosemiquinone radical intermediate that is likely accompanied by conformational change of the carboxyl-terminal region. Unexpectedly, we found that the flavosemiquinone radical intermediate was more stable at 20 °C than at 4 °C in the absence of an external electron and/or hydrogen donor, implying some involvement in physiological function(s) at avian body temperature. Thus, cCRY4 seems to be an intrinsically photosensitive and photoswitchable molecule, and may exemplify a vertebrate model of cryptochrome with possible function as a photosensor and/or magnetoreceptor.

SIGNIFICANCE STATEMENT

Cryptochromes (CRYs) function as blue light photoreceptors, circadian clock molecules, or magnetoreceptors. Non-mammalian vertebrates have CRY4 but its function is not well understood. Chicken CRY4 may be a magnetoreceptor due to its high expression in the retina and light-dependent structural changes in retinal homogenates. To examine the molecular nature of cCRY4, we developed an expression system of tagged and non-tagged cCRY4 in budding yeast. Spectroscopic and biochemical analyses of recombinant cCRY4 revealed that structural changes with light irradiation occurred through formation of a radical form. We believe that cCRY4 is one of the best models to characterize the photocycle of vertebrate cryptochrome.

INTRODUCTION

CRY and photolyase (photorepair enzyme, PL) are flavoproteins that are widely distributed in living organisms such as bacteria, fungi, plants, and animals (1). Almost all of the CRY/ PL family proteins function as photoreceptors for a variety of light-dependent physiological responses such as DNA repair (2), photomorphogenesis (3, 4), circadian clock function (5, 6), and magnetoreception (7). Similar to PL, CRY photoreaction may be composed of four steps: (i) photoexcitation of chromophore, flavin adenine dinucleotide (FAD), (ii) intramolecular electron and/or proton transfer, (iii) the conformational change of protein, and (iv) signal transduction and functional expression. Photoreaction mechanisms of plant CRY and insect type1 CRY have been studied *in vitro* and *in vivo* (8-17), yet the light-dependent redox cycling of vertebrate cryptochromes remains elusive.

Vertebrates have several classes of CRYs, among which CRY1 and CRY2 function as negative components of the circadian oscillator (18, 19). CRY4 has been found in non-mammalian vertebrates, but it lacks the circadian transcriptional regulatory function (20-22) or the photorepair activity (20). Although the molecular function(s) of CRY4 proteins are unknown, a photoreceptor and/or light-driven magnetoreceptor function have been suggested based on the following evidence: (i) CRY4 proteins retain carboxyl-terminal extension sequences called CCE regions (cryptochrome carboxyl-terminal extension region), which are not found in PLs and commonly found in CRYs (23); (ii) chicken CRY4 (cCRY4) is highly expressed in the retina (24), a postulated central site for magnetoreception (25); and (iii) cCRY4 in chicken retinal homogenates is immunoprecipitated with

higher efficiency in the dark than light by C1 mAb, which recognizes stretches of 14 amino acids (QLTRDDADDPMEMK) within the CCE region (24). Although these results, as well as a change in molecular structure in homogenate, are consistent with the idea of cCRY4 photoreception and/or magnetoreception, whether the light-dependent structural change of cCRY4 requires other factors that are endogenously expressed in the chicken retina remains unclear.

To address these unknowns and further examine the molecular nature of cCRY4, we developed an expression system of tagged and non-tagged cCRY4 in budding yeast. Spectroscopic and biochemical analyses of recombinant cCRY4 revealed that structural changes with light irradiation occurred through formation of a radical form. We also found redox- and temperature-dependency in the cCRY4 photocycle.

RESULTS

Expression of Recombinant cCRY4 in Budding Yeast

To perform molecular analysis, we developed expression systems for GST-tagged and non-tagged cCRY4 using budding yeast, and purified the recombinant cCRY4 proteins. The MaV203 strain was chosen because the cells of this yeast strain could easily be lysed by sonication. GST-cCRY4 and cCRY4 protein expression in yeast was approximately 10 mg in a 5 L culture, and we obtained after purification 354 μg of GST-cCRY4 from 10 L culture and 349 μg of non-tagged cCRY4 from 2.5 L culture (Fig. 1A, B). After overnight incubation in the dark at 4 °C, the UV-visible absorption spectra of the purified recombinant proteins were recorded and a characteristic absorption pattern of oxidized flavin binding was identified (Fig. 1C). The recombinant GST-cCRY4 sample was denatured by heat to extract the chromophore in a soluble fraction. HPLC analysis of the supernatant clearly indicated the consistent presence of FAD (Fig. 1D). Comparison of the FAD content in the extract suggested that most cCRY4 proteins in the sample were bound to FAD at a molar ratio of 1:1.

Light-induced Structural Change Involving CCE of Recombinant cCRY4

Recombinant cCRY4 was immunoprecipitated under dark or blue light conditions to decipher whether there was a light-dependent interaction with C1 mAb (Fig. 2). The relative amount of recombinant cCRY4 immunoprecipitated under light conditions (L in Fig. 2B) was significantly lower than that under dark conditions (D in Fig. 2B), indicating that recombinant cCRY4 receives a photon

without any factor(s) that change its CCE structure. These results suggest that associating factor(s) in the chicken retina are not required for cCRY4 photoreceptive properties.

Light-dependent Change in Tryptic Digestion Sensitivity of cCRY4

To reveal whether the light-dependent dissociation of GST-cCRY4 from C1-mAb was associated with a CCE-specific structural change or an entire conformational change, we performed partial proteolysis of GST-cCRY4 (Fig. 3). Upon partial tryptic digestion, the immunopositive band for full-length GST-cCRY4 (F1, Fig. 3A, lane1) disappeared, and F2~F6 fragments appeared (Fig. 3A, lane 3). Since the C1 mAb epitope localized within CCE, the F2 band (approx. 61 kDa) likely corresponds to cCRY4 generated by trypsin cleavage around the linker region between GST and cCRY4 (Fig. 3B). Just below the bands for the F2 fragments, F3 fragments (approx. 58 kDa) were detected regardless of the lighting conditions. Signals for F4 (approx. 32 kDa), F5 (approx. 30 kDa) and F6 (approx. 26 kDa) bands were noticeably stronger when GST-CRY4 was digested by trypsin in the dark versus the light (Fig. 3A).

Photic Absorbance Changes of cCRY4

After overnight incubation in the dark at 4 °C, when placed in 20 °C temperatures and regardless of the presence of 5 mM DTT, cCRY4 showed an absorption pattern characteristic of the CRY/PL family proteins with an oxidized FAD chromophore (FAD_{ox} form). Upon blue light irradiation (453 nm, 1 mW/cm^2) in the presence of DTT, absorption peaks at around 370 nm and 447 nm showed a decrease within 0.5 min, and the peak at around 500-650 nm showed an increase, most likely due to photic generation of a semiquinone radical intermediate having $FADH^{\bullet}$ chromophore ($FADH^{\bullet}$ form) from the FAD_{ox} form (Fig. 4A, B). Further irradiation induced a decrease in the absorption bands at around 370 nm, 447 nm, and 500-650 nm (Fig. 4A and 4B, curves 1 min-8 min). We believe the absorption decrease in the longer wavelength regions was most likely due to a reduction of $FADH^{\bullet}$ to its fully reduced $FADH^{-}$ form since such change was not observed when the semiquinone radical intermediate was incubated in the dark (Fig. S1A).

Enhancement of Photic Formation of $FADH^{\bullet}$ by DTT

To investigate the effect of reducing agent DTT on photoreduction of the FAD chromophore, we compared the cCRY4 photocycle in both the presence (5 mM) and absence of DTT at 20 °C and 4 °C

(Fig. 4). When $FADH^{\bullet}$ formation was monitored by a decrease in the FAD_{ox} form, the reaction proceeded even in the absence of DTT (Fig. 4C, D), but the formation of $FADH^{\bullet}$ was about 1.6 times slower than when in the presence of 5 mM DTT at 20 °C (Fig. 4E). Although DTT enhancement of the formation of $FADH^{\bullet}$ was observed, we could not find an obvious temperature dependency related to $FADH^{\bullet}$ formation in our experiment.

Extended blue light irradiation (～32 min) in the absence of DTT did not photoreduce $FADH^{\bullet}$ to $FADH^{-}$ as shown by the absorption changes at around 500-650 nm. Therefore, chromophore reduction from $FADH^{\bullet}$ to $FADH^{-}$ seemed to be suppressed in the absence of external reducing agents. Interestingly, photoreduction from $FADH^{\bullet}$ to $FADH^{-}$ in the absence of DTT was slower at 20 °C than 4 °C (Fig. 4F), while such temperature dependency was not observed in the presence of DTT (Fig. 4F).

Photic Reaction of $FADH^{\bullet}$ and Photocycle of cCRY4

In the case of *Chlamydomonas reinhardtii* CRYa (26, 27), red light irradiation of $FADH^{\bullet}$ also resulted in the formation of $FADH^{-}$ form; therefore, we examined the long-wavelength sensitivity of $FADH^{\bullet}$ in cCRY4 (Fig. 5). There was decreased absorption at around 500-650 nm with red light irradiation of $FADH^{\bullet}$ (Fig. 5A, B). In this case, absorption changes in the shorter wavelength region (300-500 nm) were minimal and quite different from those observed when $FADH^{\bullet}$ was oxidized to FAD_{ox} in dark conditions (Fig. S1). Simultaneous irradiation with both short-wavelength and long-wavelength light using a white LED resulted in the direct reduction of FAD_{ox} to $FADH^{-}$ (Fig. 5C), which supports the idea that $FADH^{\bullet}$ was reduced to $FADH^{-}$ with long-wavelength light irradiation.

When taking the different absorption spectra of cCRY4 (Fig. 5B) and those reported for *C. reinhardtii* CRYa into consideration, we concluded that the $FADH^{\bullet}$ form in cCRY4 was reduced to $FADH^{-}$ with red light irradiation as was the case with *C. reinhardtii* CRYa. We estimated the absolute absorbance spectra of FAD_{ox}, $FADH^{\bullet}$ and $FADH^{-}$ forms using the different absorption spectra obtained in our present measurements (Fig. 5D).

Light-dependent Structural Change of cCRY4 Occurs during Photoreduction of FAD_{ox} to $FADH^{\bullet}$

As a first step in understanding the intra-molecular photoreception mechanism of cCRY4, we examined whether the light-dependent structural change of cCRY4 occured in $FADH^{\bullet}$ by comparing

temporal profiles of the structural and spectroscopic changes (Fig. 6). Chick retinal homogenates were incubated in the dark on a C1-mAb-immobilized gel to immunoprecipitate cCRY4, and then the gel was irradiated with blue light (470 nm, 100 mW/cm^2). The amount of cCRY4 that dissociated from the C1 mAb-cCRY4 immunocomplex was measured using immunoblot analysis of the supernatants recovered at various time points. Retinal cCRY4 was released from the C1 mAb-gel within 0.75 min, which is the time point when the FADH$^\bullet$ form is produced, not the fully reduced form (Fig. 6). The estimated time course of their dissociation (Fig. 6B, closed circles) was similar to that for FADH$^\bullet$ accumulation measured by spectroscopy (Fig. 6B, open squares). These results suggest that light-induced structural change in cCRY4 occurs during or just after reduction of the FAD_{ox} chromophore.

DISCUSSION

Overexpression and Purification of Chicken CRY4

In this study, we report a novel constitutive expression system for cCRY4 in budding yeast MaV203. In preliminary experiments, we tried to overexpress recombinant cCRY4 in *Escherichia coli* and insect cells, but we could not obtain a sufficient amount of cCRY4 protein for spectroscopic analysis. The baculovirus expression system is conventionally used for the expression of recombinant CRY proteins (8, 10, 11, 28), and there are a couple reports of systems using yeast cells in which the expression of exogenous proteins could be induced in *Schizosaccharomyces pombe* (29) and *Pichia pastoris* (30). We believe our novel constitutive expression system may be more convenient than other systems due to the ease with which it can be scaled up for preparation of large amounts of CRY proteins.

Light-induced Reduction of FAD Chromophore

While both GST-tagged and non-tagged cCRY4 likely bound FAD chromophore (Fig. 1), we chose to use non-tagged cCRY4 for further spectroscopic analysis (Fig. 4 and 5). Blue light irradiation of the FAD_{ox} form of cCRY4 caused the generation of FADH$^\bullet$ with absorption bands at around 500-650 nm, followed by chromophore photoreduction to FADH$^-$ with extended blue light (Fig. 4A-D) or red light irradiation (Fig. 5).

Notably, DTT enhanced the formation of FADH$^\bullet$ from FAD_{ox} (Fig. 4E). To our knowledge, DTT enhancement of the radical formation has not been reported for any of the CRYs, even though

spectroscopic analyses of CRY/PL proteins have been performed in the presence of DTT. In a previous study on *Chlamydomonas reinhardtii* CRY (26), DTT did not exhibit any effects on the blue light-induced formation of $FADH^{\bullet}$ from the FAD_{ox} form, while DTT did enhance the formation of $FADH^{-}$ from the $FADH^{\bullet}$ form. Beel et al. explained that in their investigation the primary reduction of FAD_{ox} likely involved an electron (or hydrogen) donor present in the protein itself. In the case of cCRY4, we propose that DTT may attack the FAD_{ox} chromophore more readily than an intrinsic electron and/or hydrogen donor would.

While the primary photoreduction step was enhanced by DTT and was temperature-independent (Fig. 4E), the secondary photoreduction step (the formation of $FADH^{-}$ from the $FADH^{\bullet}$ form, Fig. 4F) was affected by both DTT and temperature. The formation of $FADH^{-}$ was noticeably slower at 20 °C than at 4 °C in the absence of DTT. In cases where there is no external electron donor around cCRY4, an intrinsic electron donor may play a role in the reduction of $FADH^{\bullet}$. Therefore, we believe there is temperature-dependent conformational change for chromophore reduction and that this may increase the distance between the intraprotein electron donor and the chromophore at higher temperatures. Considering that the photoreduction of $FADH^{\bullet}$ is suppressed by raising the temperature, the $FADH^{\bullet}$ form of cCRY4 may be stable at higher temperatures (e.g. avian body temperature). Taking into account that cCRY4 changes its conformation during or after the reduction of FAD_{ox} to $FADH^{\bullet}$ (Fig. 6), this long-lived radical form may play a role in cCRY4 functions such as phototransduction or magnetoreception. Alternatively, there could be unknown intrinsic factors that oxidize $FADH^{\bullet}$ for rapid inactivation in the retinal cells.

Light-induced Structural Change of cCRY4

We demonstrated in a previous study that the interaction between retinal cCRY4 and C1 mAb changes in a light-dependent manner (24). While this may mean that light initiates a dynamic structural change that includes CCE, there is still the possibility that a retinal factor locally modifies the C1 epitope in CCE and alters immunoreactivity to C1 mAb with light irradiation. Another possibility is that other retinal phototransduction proteins such as the opsins or rhodopsin kinase assist with photic changes. The present study was undertaken using recombinant cCRY4 protein without retinal factor(s). Based on our results, we concluded that cCRY4 itself retained photosensitivity to change its structure dynamically during photic changes with immunoprecipitation (Fig. 2) and protease-resistance (Fig. 3).

The light-dependent change in trypsin resistance (Fig. 3) led us to infer a possible site for the structural changes. Because the C1 mAb epitope is located within close proximity of the C-terminus, we were able to map putative trypsin cleavage sites that could produce F4-F6 fragments. Those sites with trypsin resistance only in light were mapped at a region close to the FAD-binding domain within the PHR (See Fig. 3C blue region; predicted cCRY4 3D structure with the aid of MATRAS using structural data for *Arabidopsis thaliana* (6-4) photolyase (PDB acc. No. 3fy4B) as the template). This region may be highly accessible to trypsin in the dark and less accessible in the light. Such change in the accessibility resembles that of C1 mAb to its epitope in the CCE region (Red-colored region in Fig. 3C). Moreover, these two regions are mapped distant from each other in the putative 3D model, and hence one plausible explanation is that the CCE region may move to bind to the FAD-binding domain in the light, which makes it more difficult for trypsin and C1-mAb to access the FAD-binding domain and C1-mAb epitope, respectively.

Previous studies on *Arabidopsis thaliana* CRY1 (AtCRY1) and the *Drosophila melanogaster* CRY (dCRY) reported that the CCE and PHR of these CRYs bind together in the dark and dissociate with light irradiation (12, 14, 31, 32). The light-dependent dissociation enables binding with COP1 or JETLAG, downstream signaling molecules for AtCRY1 and dCRY, respectively (14, 33), and triggers the phototransduction cascade. Considering that cCRY4 is opposite in nature in that the CCE region seems to bind with PHR with a light signal, a possible downstream effector for cCRY4 may bind to cCRY4 in the dark. Future investigation of molecules that interact with cCRY4 would help to better understand the physiological functions of cCRY4.

Photocycle of cCRY4

Short durations of cCRY4 irradiation with blue light reduced the FAD_{ox} chromophore to $FADH^{\bullet}$. Extended durations of irradiation further reduced $FADH^{\bullet}$ to the $FADH^{-}$ form (Fig. 4, 5). Both forms returned to FAD_{ox} in the dark (Fig. S1), closing the photocycle depicted in Fig. 7. Oztürk et al. obtained FLAG-tagged cCRY4 by using a baculovirus system, and they investigated photic reduction of the FAD_{ox} form to $FADH^{-}$ (or $FADH_2$) using irradiation comprised of relatively strong UV-A (366 nm, 2 mW/cm^2) for 10 min (28). They additionally observed only reoxidation from $FADH^{-}$ to stable $FADH^{\bullet}$ during 5 hours of incubation in the dark. Although their observations are not congruent with the photocyle shown in Fig. 7, there are many differences in experimental conditions such as the expression system used, the presence of FLAG-tag, and different irradiation wavelengths (UV-A or

blue light). The speculated photocycle of cCRY4 (Fig. 7) is similar to that of AtCRY1 (8), but in the case of AtCRY1, $FADH^{\bullet}$ was not detected spectroscopically when $FADH^{-}$ was incubated in the dark for reoxidation to FAD_{ox} (34). This may be due to the rapid oxidization of $FADH^{\bullet}$ to FAD_{ox} in the two-electron reoxidation process of AtCRY1.

In the present study, both the $FADH^{\bullet}$ and $FADH^{-}$ forms of cCRY4 were oxidized *in vitro* under dark conditions (Fig. S1). A recent study on chicken CRY1a (cCRY1a) (35), another CRY identified in the chicken retina, implied that cCRY1a may absorb not only blue light but also that of longer wavelengths (e.g. green, yellow) utilizing the $FADH^{\bullet}$ state and changing its CCE conformation in the $FADH^{-}$ state. Nießner et al. analyzed cCRY1a activation using the chicken retina *in vivo*; therefore, future investigation extending our novel yeast expression system to other CRY proteins both *in vivo* and *in vitro* may be beneficial to further analyses.

Biological Functions of CRY4

Avian CRYs are speculated to work as light-driven magnetoreceptors (25) based on their localization in the retina (24, 36, 37) and the photosensitivity of the purified protein (38, 39). On the other hand, in the Western clawed frog, CRY4 is highly expressed in the ovary and testis rather than the retina (22) and hence more likely to be implicated in unknown photic function(s) in the gonadal tisses instead of magnetoreception. Considering that CRY involves multiple functions such as nonvisual photoreception (5, 40), magnetoreception (7) and vision (41), CRY4 may play multiple roles in different cells and/or organs.

MATERIALS AND METHODS

Materials and methods are reported in *SI Materials and Methods*. Described therein are protocols followed for protein expression and purification, UV-visible spectroscopy, HPLC analysis, immunoprecipitation, and partial proteolysis.

FOOTNOTES

Author contributions: H.M., T.M., C.Y., Y.T., R.W., Y.K., K.O., and T.O. designed and performed research, and analyzed data; and H.M. and T.O. wrote the paper.

The authors declare no conflict of interest.

This article is a PNAS Direct Submission.

[1]To whom correspondence should be addressed: E-mail: okano@waseda.jp

ACKNOWLEDGEMENTS

This work was partially supported by the Grants-in-Aid from the Ministry of Education, Culture, Sports, Science and Technology (MEXT), the Research Foundation for Opto-Science and Technology, and the Japanese Society for the Promotion of Science (JSPS, No.23248033, 24657109, 26650024) of Japan awarded to T. O.

REFERENCES

1. Cashmore AR (2003) Cryptochromes: enabling plants and animals to determine circadian time. *Cell* 114(5):537-543.
2. Brettel K & Byrdin M (2010) Reaction mechanisms of DNA photolyase. *Curr Opin Struct Biol* 20(6):693-701.
3. Ahmad M & Cashmore AR (1993) *HY4* gene of *A. thaliana* encodes a protein with characteristics of a blue-light photoreceptor. *Nature* 366(6451):162-166.
4. Guo H, Yang H, Mockler TC, & Lin C (1998) Regulation of flowering time by Arabidopsis photoreceptors. *Science* 279(5355):1360-1363.
5. Emery P, So WV, Kaneko M, Hall JC, & Rosbash M (1998) CRY, a Drosophila clock and light-regulated cryptochrome, is a major contributor to circadian rhythm resetting and photosensitivity. *Cell* 95(5):669-679.
6. Hirayama J*, et al.* (2009) Common light signaling pathways controlling DNA repair and circadian clock entrainment in zebrafish. *Cell Cycle* 8(17):2794-2801.
7. Gegear RJ, Casselman A, Waddell S, & Reppert SM (2008) Cryptochrome mediates light-dependent magnetosensitivity in Drosophila. *Nature* 454(7207):1014-1018.
8. Lin C*, et al.* (1995) Association of flavin adenine dinucleotide with the Arabidopsis blue light receptor CRY1. *Science* 269(5226):968-970.
9. Giovani B, Byrdin M, Ahmad M, & Brettel K (2003) Light-induced electron transfer in a cryptochrome blue-light photoreceptor. *Nat Struct Biol* 10(6):489-490.
10. Banerjee R*, et al.* (2007) The signaling state of Arabidopsis cryptochrome 2 contains flavin semiquinone. *J Biol Chem* 282(20):14916-14922.
11. Berndt A*, et al.* (2007) A novel photoreaction mechanism for the circadian blue light photoreceptor Drosophila cryptochrome. *J Biol Chem* 282(17):13011-13021.
12. Kondoh M*, et al.* (2011) Light-induced conformational changes in full-length Arabidopsis thaliana cryptochrome. *J Mol Biol* 413(1):128-137.
13. Li X*, et al.* (2011) Arabidopsis cryptochrome 2 (CRY2) functions by the photoactivation mechanism distinct from the tryptophan (trp) triad-dependent photoreduction. *Proc Natl Acad Sci USA* 108(51):20844-20849.
14. Ozturk N, Selby CP, Annayev Y, Zhong D, & Sancar A (2011) Reaction mechanism of Drosophila cryptochrome. *Proc Natl Acad Sci USA* 108(2):516-521.

15. Vaidya AT*, et al.* (2013) Flavin reduction activates Drosophila cryptochrome. *Proc Natl Acad Sci USA* 110(51):20455-20460.

16. Ozturk N, Selby CP, Zhong D, & Sancar A (2014) Mechanism of photosignaling by Drosophila cryptochrome: role of the redox status of the flavin chromophore. *J Biol Chem* 289(8):4634-4642.

17. Muller P*, et al.* (2014) ATP binding turns plant cryptochrome into an efficient natural photoswitch. *Sci Rep* 4:5175.

18. Kume K*, et al.* (1999) mCRY1 and mCRY2 are essential components of the negative limb of the circadian clock feedback loop. *Cell* 98(2):193-205.

19. Yamamoto K, Okano T, & Fukada Y (2001) Chicken pineal Cry genes: light-dependent up-regulation of cCry1 and cCry2 transcripts. *Neurosci Lett* 313(1-2):13-16.

20. Kobayashi Y*, et al.* (2000) Molecular analysis of zebrafish photolyase/cryptochrome family: two types of cryptochromes present in zebrafish. *Genes Cells* 5(9):725-738.

21. Kubo Y, Akiyama M, Fukada Y, & Okano T (2006) Molecular cloning, mRNA expression, and immunocytochemical localization of a putative blue-light photoreceptor CRY4 in the chicken pineal gland. *J Neurochem* 97(4):1155-1165.

22. Takeuchi T, Kubo Y, Okano K, & Okano T (2014) Identification and characterization of cryptochrome4 in the ovary of western clawed frog Xenopus tropicalis. *Zoolog Sci* 31(3):152-159.

23. Ozturk N*, et al.* (2007) Structure and function of animal cryptochromes. *Cold Spring Harb Symp Quant Biol* 72:119-131.

24. Watari R*, et al.* (2012) Light-dependent structural change of chicken retinal Cryptochrome4. *J Biol Chem* 287(51):42634-42641.

25. Ritz T, Adem S, & Schulten K (2000) A model for photoreceptor-based magnetoreception in birds. *Biophys J* 78(2):707-718.

26. Beel B*, et al.* (2012) A flavin binding cryptochrome photoreceptor responds to both blue and red light in Chlamydomonas reinhardtii. *Plant Cell* 24(7):2992-3008.

27. Spexard M, Thoing C, Beel B, Mittag M, & Kottke T (2014) Response of the Sensory animal-like cryptochrome aCRY to blue and red light as revealed by infrared difference spectroscopy. *Biochemistry* 53(6):1041-1050.

28. Ozturk N*, et al.* (2009) Comparative photochemistry of animal type 1 and type 4

cryptochromes. *Biochemistry* 48(36):8585-8593.

29. Sang Y, *et al.* (2005) N-terminal domain-mediated homodimerization is required for photoreceptor activity of Arabidopsis CRYPTOCHROME 1. *Plant Cell* 17(5):1569-1584.
30. Vieira J, *et al.* (2012) Human cryptochrome-1 confers light independent biological activity in transgenic Drosophila correlated with flavin radical stability. *PLoS One* 7(3):e31867.
31. Partch CL, Clarkson MW, Ozgur S, Lee AL, & Sancar A (2005) Role of structural plasticity in signal transduction by the cryptochrome blue-light photoreceptor. *Biochemistry* 44(10):3795-3805.
32. Levy C, *et al.* (2013) Updated structure of Drosophila cryptochrome. *Nature* 495(7441):E3-4.
33. Liu H, Liu B, Zhao C, Pepper M, & Lin C (2011) The action mechanisms of plant cryptochromes. *Trends Plant Sci* 16(12):684-691.
34. Muller P & Ahmad M (2011) Light-activated cryptochrome reacts with molecular oxygen to form a flavin-superoxide radical pair consistent with magnetoreception. *J Biol Chem* 286(24):21033-21040.
35. Niessner C, *et al.* (2013) Magnetoreception: activated cryptochrome 1a concurs with magnetic orientation in birds. *J R Soc Interface* 10(88):20130638.
36. Mouritsen H, *et al.* (2004) Cryptochromes and neuronal-activity markers colocalize in the retina of migratory birds during magnetic orientation. *Proc Natl Acad Sci USA* 101(39):14294-14299.
37. Niessner C, *et al.* (2011) Avian ultraviolet/violet cones identified as probable magnetoreceptors. *PLoS One* 6(5):e20091.
38. Liedvogel M, *et al.* (2007) Chemical magnetoreception: bird cryptochrome 1a is excited by blue light and forms long-lived radical-pairs. *PLoS One* 2(10):e1106.
39. Du XL, *et al.* (2014) Observation of magnetic field effects on transient fluorescence spectra of cryptochrome 1 from homing pigeons. *Photochem Photobiol* 90(5):989-996.
40. Tu DC, Batten ML, Palczewski K, & Van Gelder RN (2004) Nonvisual photoreception in the chick iris. *Science* 306(5693):129-131.
41. Mazzotta G, *et al.* (2013) Fly cryptochrome and the visual system. *Proc Natl Acad Sci USA* 110(15):6163-6168.

FIGURE LEGENDS

FIGURE 1. Expression in yeast, purification, and chromophore characterization of recombinant cCRY4.

SDS-PAGE analysis and CBB staining of purified (A) GST-cCRY4 (calculated molecular weight: 88,094 Da) and (B) non-tagged cCRY4 (calculated molecular weight: 61,063 Da). C. UV-visible absorption spectra of GST-cCRY4 (solid line) and non-tagged cCRY4 (dashed line). (Inset) Photograph of the purified yellow-colored GST-cCRY4 protein (708 mg/ml). D. HPLC analysis of GST-cCRY4 chromophore. Detailed protocol is described in Experimental Procedures.

FIGURE 2. Light-dependent CCE structural change of GST-cCRY4.

A. Schematic drawing of the immunoprecipitation assay of GST-cCRY4. Purified GST-cCRY4 (in buffer containing 21.5 mM Tris-HCl, pH 7.5, 147.5 mM NaCl, 0.95 mM DTT, 9.5% (v/v) glycerol, 0.095% Tween20, Complete EDTA free protease inhibitor mixture (Roche Applied Sciences)) and C1-mAb-gel were mixed, and an immunoprecipitation reaction was performed at 4 °C and 16 hours under light (L: 470 nm, 424 mW/cm^2) or dark (D: covered with aluminum foil) conditions. B. Immunoblot analysis of immunoprecipitants and supernatants. Immunoprecipitation reaction, recovering the supernatants, and washing of the C1-mAb-gel were performed under the indicated light conditions. Relative immunoprecipitated level of GST-cCRY4 was calculated by dividing the signal intensity of ppt by that of sup plus ppt (n = 3)。Error bars represent standard deviation. *$p<0.05$ (Student's *t*-test) C1, C1 mAb which recognizes the carboxyl terminal region of cCRY4 (Gln494-Lys507). C3, C3 mAb which recognizes the carboxyl terminal region of cCRY4 (His512-Met525).

FIGURE 3. Partial proteolysis of GST-cCRY4 by trypsin under light or dark conditions.

A. Tryptic digestion of GST-cCRY4 in the presence of 5 mM DTT under Light (352 nm, 1 mW/cm^2) and Dark (covered with aluminum foil) conditions. Tryptic digests are labeled F1-F6. B. Estimated trypsin-digestion sites in GST-cCRY4 primary structure. The approximate molecular weight of fragments are F1: 79 kDa, F2: 61 kDa, F3: 58 kDa, F4: 32 kDa, F5: 30 kDa, and F6: 26 kDa. Calculated molecular weight of GST-cCRY4, 88,094 Da. C1, C1-mAb epitope. C. Trypsin-digestion sites in a predicted cCRY4 3D structure. Predicted light-dependent tryptic

digestion sites (green-colored amino acids in the blue-colored region) and the C1-mAb epitope (red-colored region) are indicated. A simple sequence replacement model of cCRY4 (Phe9-Glu515) was constructed based on *Arabidopsis thaliana* (6-4) PL (PDB acc. No. 3fy4B) with the aid of MATRAS server.

FIGURE 4. Blue light-induced spectral change of non-tagged cCRY4.

A. Spectral changes of cCRY4 caused by blue light irradiation (0.5-8 min, 453 nm, 1 mW/cm^2) in the presence of 5 mM DTT. B. Light minus dark differences in absorption spectra of cCRY4 in the presence of 5 mM DTT. C. Spectral changes of cCRY4 caused by blue light irradiation (0.5-32 min, 455 nm, 1 mW/cm^2) in the absence of DTT. D. Light minus dark differences in the absorption spectra of cCRY4 in the absence of DTT. E. Effects of temperature and DTT on the formation of cCRY4 FADH$^\bullet$ monitored by the difference in absorbance at 447 nm. F. Effects of temperature and DTT on the formation of cCRY4 FADH$^-$ monitored by the difference in absorbance at 630 nm.

FIGURE 5. Red light reduced FADH$^\bullet$ to FADH$^-$ in non-tagged cCRY4.

A. Absorbance changes of FADH$^\bullet$ in cCRY4 upon red light irradiation (628 nm, 0.7 mW/cm^2). FADH$^\bullet$ was generated by 0.5 min of blue light irradiation of the FAD$_{ox}$ form followed by red light irradiation (0.5-32 min). B. Differences in absorption spectra before and after red light irradiation (red minus blue) are plotted. C. Absorption spectra before and after white light irradiation (128 min) of the FAD$_{ox}$ form, showing photoconversion from FAD$_{ox}$ to FADH$^-$ without the accumulation of FADH$^\bullet$. D. Absolute absorbance spectra of cCRY4 photointermediates estimated by calculation. The dark-adapted samples ("dark" in panel A and "dark" in panel C) are considered to be mainly composed of FAD$_{ox}$ with a small amount of residual FADH$^\bullet$. The sample, after long irradiation with white light ("white_128 min" in panel C), is presumed to be composed of only FADH$^-$ forms. Spectral changes induced by the initial 0.5 min blue light and the following 8 min red light irradiations are assumed to correspond to conversions from FAD$_{ox}$ to FADH$^\bullet$ and FADH$^\bullet$ to FADH$^-$, respectively. The absorbance spectra were estimated using the spectra of "dark", "blue_0.5 min", and "red_8 min" in panel A, and "dark" and "white_128 min" in panel C as follows: [i] All spectra were normalized by their optical density and presumed to have absorbances at the peak of the dark-adapted spectrum such that the FAD$_{ox}$ form (447 nm) was 1.0. Absorbances at putative isosbestic points between the FADH$^\bullet$ and FADH$^-$ forms (446 nm, red_8 min in panel B) or the FAD$_{ox}$

and $FADH^{\bullet}$ forms were used (388 nm, panel C). [ii] Changing the putative photobleaching rates of FAD_{ox} from 20-50%, putative absolute absorption spectra for $FADH^{\bullet}$ were calculated and the photobleaching rate was determined to be 29.5% placing the isosbestic point between $FADH^{\bullet}$ and $FADH^{-}$ at 446 nm. [iii] The determined absolute absorption spectrum of $FADH^{\bullet}$ was diminished from "dark" or "white_128 min" in the panel C spectrum with changing putative contents of the contaminating $FADH^{\bullet}$ form. We inferred the $FADH^{\bullet}$ content in the FAD_{ox} and $FADH^{-}$ forms to be 3% and 0%, respectively, on the assumption that FAD_{ox} had no absorbance in the longer wavelength region (> 520 nm).

FIGURE 6. *In vitro* comparative analysis of time courses for the structural and spectral changes of recombinant cCRY4.

A. Schematic drawing of the assay. B. Time courses of the dissociation of retinal cCRY4 from C1 mAb and generation of $FADH^{\bullet}$ from FAD_{ox} upon blue-light irradiation of recombinant non-tagged cCRY4. Immunoprecipitation of chick retinal cCRY4 using C1 mAb was performed according to the experimental procedure described in (22). In brief, chick retinas were homogenized in lysis buffer containing 1 mM DTT (detailed composition of the buffer is described in (22)), and the immunocomplex containing cCRY4 was precipitated from the retinal extract with C1 mAb in the dark and irradiated with blue light (470 nm, 100 mW/cm^2) for 0.75, 1.5, 3.0, and 6.0 min. Then the amounts of cCRY4 recovered in supernatants were estimated by immunoblot analysis using C1 mAb. Representative examples of cCRY4 immunoblot signals at each time point are shown above the plot. Black circles: signal intensity of cCRY4 recovered in supernatant. Quantification of signal intensity was performed using ImageQuantTL (GE healthcare) software. Error bars represent the standard deviation of the mean. Open squares: cCRY4 absorbance changes at 630 nm during blue light (466 nm, 100 mW/cm^2) irradiation under the same buffer conditions except that protease inhibitors were omitted.

FIGURE 7. A model for cCRY4 photocycle.

Short duration (0.5 min) irradiation with blue light (453 nm, 1 mW/cm^2) reduced FAD_{ox} chromophore to the $FADH^{\bullet}$ form. Extended blue light or red light irradiation further reduced $FADH^{\bullet}$ to $FADH^{-}$. $FADH^{\bullet}$ is likely oxidized to FAD_{ox} directly in dark, while $FADH^{-}$ is likely oxidized to FAD_{ox} via $FADH^{\bullet}$ during dark incubation.

Figure 1

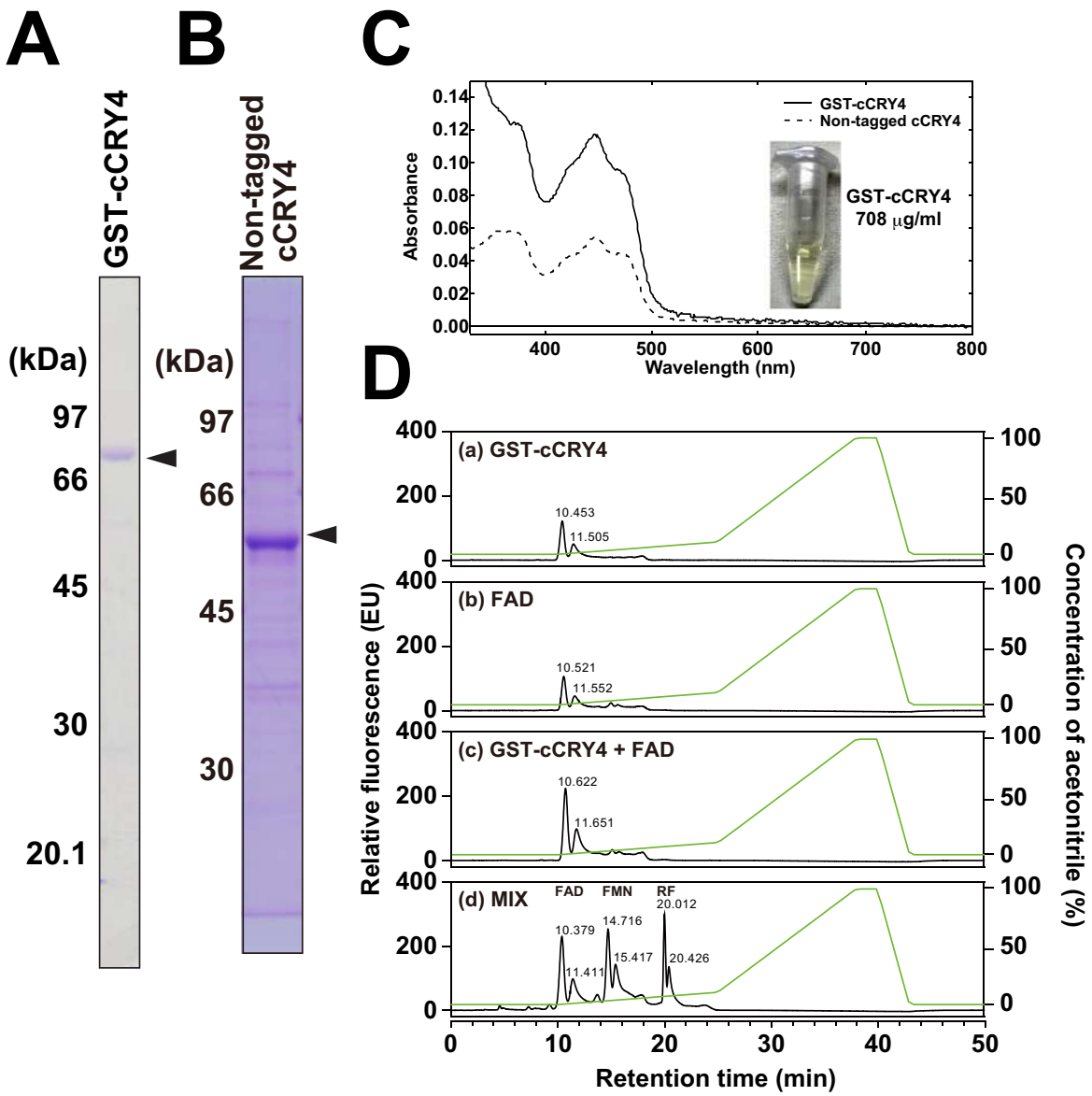
A
B
C
D
GST-cCRY4
Non-tagged cCRY4
(kDa)
97
66
45
30
20.1
Absorbance
Wavelength (nm)
GST-cCRY4
Non-tagged cCRY4
GST-cCRY4
708 μg/ml
(a) GST-cCRY4
10.453
11.505
(b) FAD
10.521
11.552
(c) GST-cCRY4 + FAD
10.622
11.651
(d) MIX
FAD
FMN
RF
10.379
11.411
14.716
15.417
20.012
20.426
Relative fluorescence (EU)
Concentration of acetonitrile (%)
Retention time (min)

Figure 2

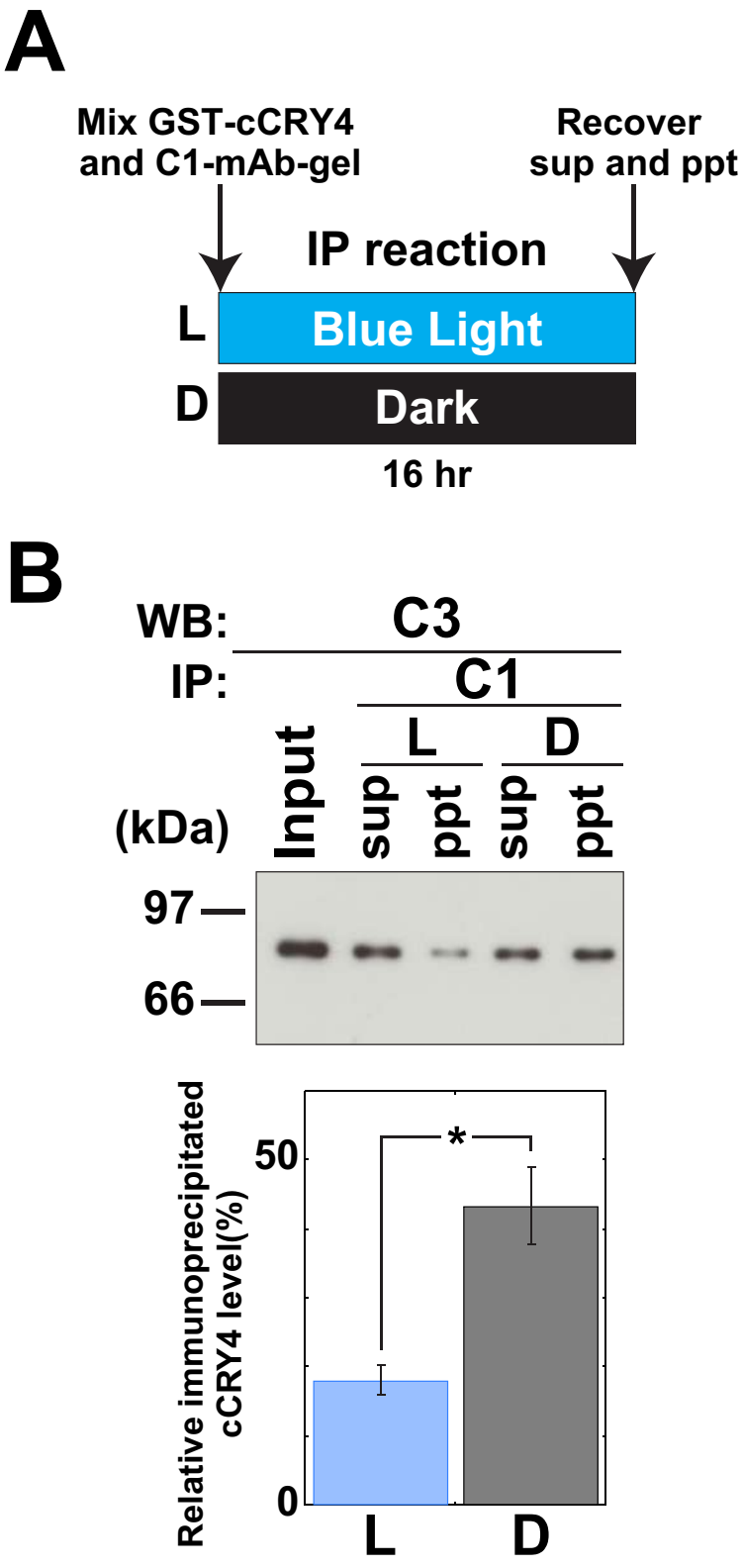
A
Mix GST-cCRY4
and C1-mAb-gel
Recover
sup and ppt
IP reaction
L
Blue Light
D
Dark
16 hr
B
WB:
C3
IP:
C1
L
D
Input
sup
ppt
sup
ppt
(kDa)
97
66
Relative immunoprecipitated
cCRY4 level(%)
50
0
*
L
D

Figure 3

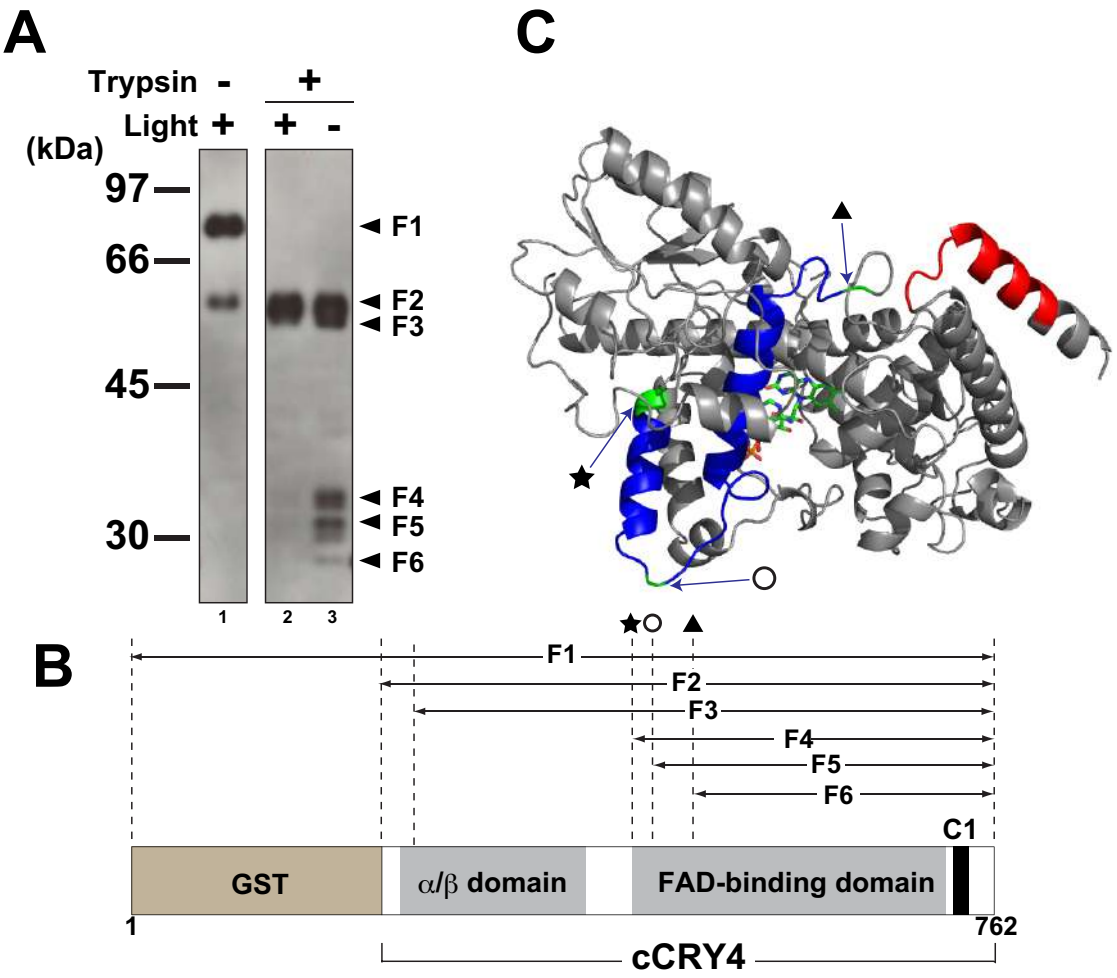
A
Trypsin - +
Light + + -
(kDa)
97
66
45
30
F1
F2
F3
F4
F5
F6
1 2 3
C
B
F1
F2
F3
F4
F5
F6
C1
GST
α/β domain
FAD-binding domain
1
762
cCRY4

Figure 4

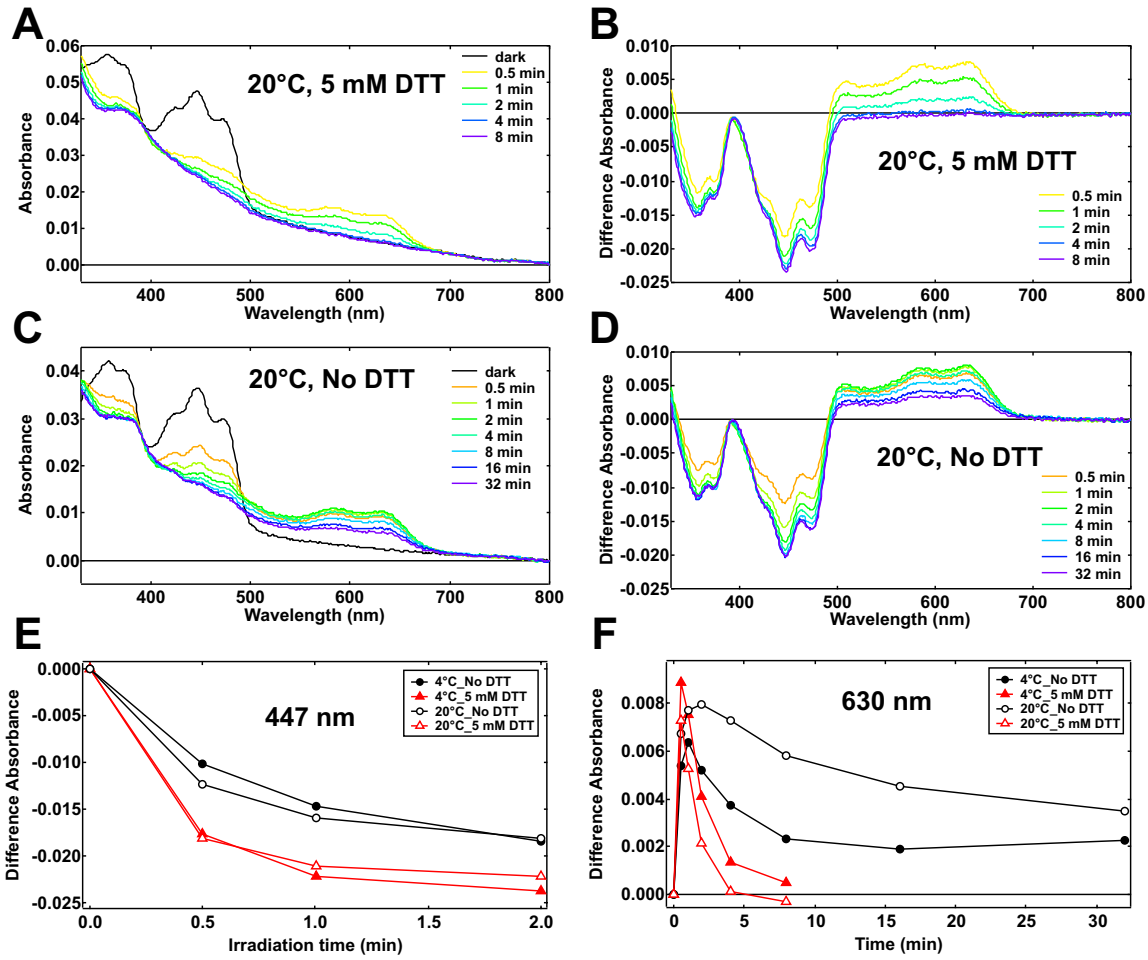
A
20°C, 5 mM DTT
dark
0.5 min
1 min
2 min
4 min
8 min
Absorbance
Wavelength (nm)
B
20°C, 5 mM DTT
0.5 min
1 min
2 min
4 min
8 min
Difference Absorbance
Wavelength (nm)
C
20°C, No DTT
dark
0.5 min
1 min
2 min
4 min
8 min
16 min
32 min
Absorbance
Wavelength (nm)
D
20°C, No DTT
0.5 min
1 min
2 min
4 min
8 min
16 min
32 min
Difference Absorbance
Wavelength (nm)
E
447 nm
4°C_No DTT
4°C_5 mM DTT
20°C_No DTT
20°C_5 mM DTT
Difference Absorbance
Irradiation time (min)
F
630 nm
4°C_No DTT
4°C_5 mM DTT
20°C_No DTT
20°C_5 mM DTT
Difference Absorbance
Time (min)

Figure 5

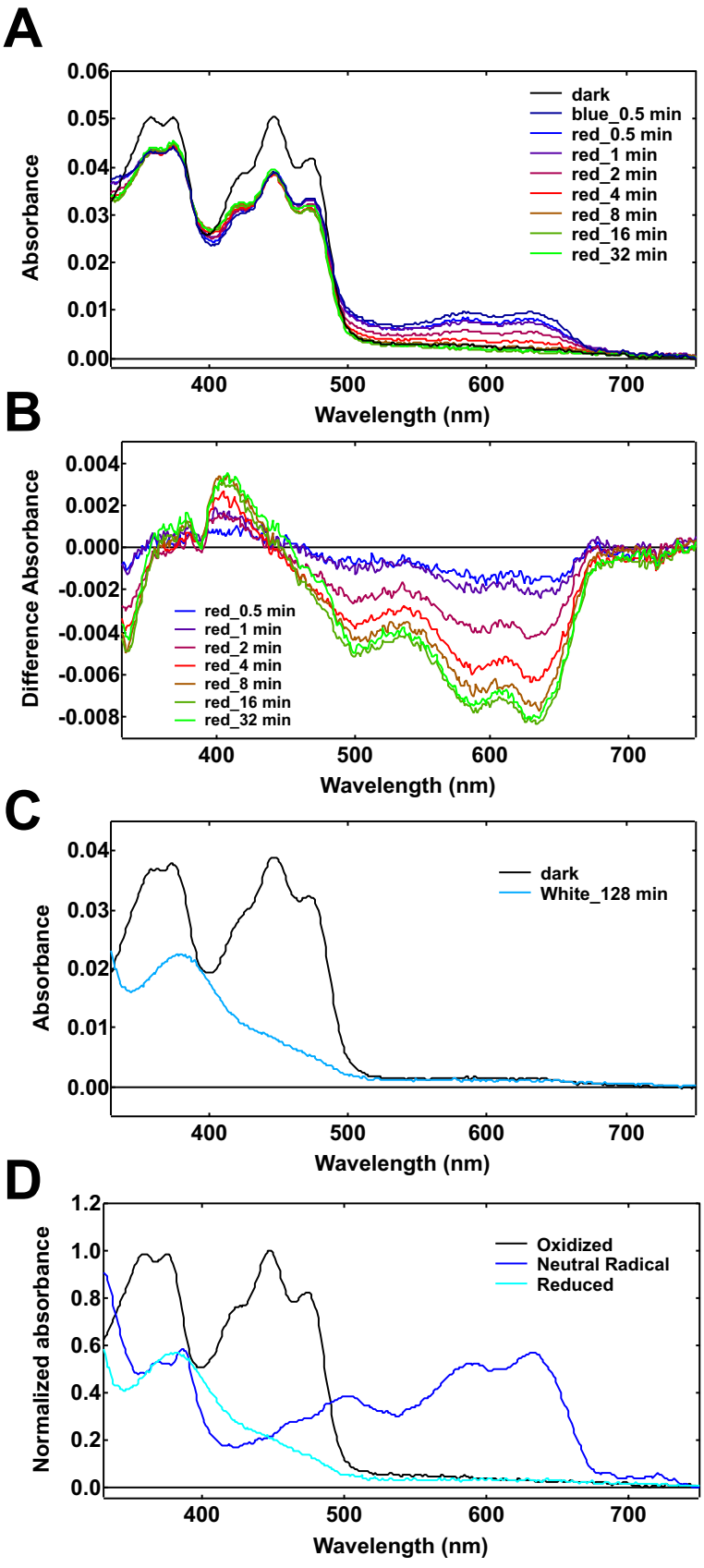
A
Absorbance
Wavelength (nm)
dark
blue_0.5 min
red_0.5 min
red_1 min
red_2 min
red_4 min
red_8 min
red_16 min
red_32 min
B
Difference Absorbance
Wavelength (nm)
red_0.5 min
red_1 min
red_2 min
red_4 min
red_8 min
red_16 min
red_32 min
C
Absorbance
Wavelength (nm)
dark
White_128 min
D
Normalized absorbance
Wavelength (nm)
Oxidized
Neutral Radical
Reduced

Figure 6

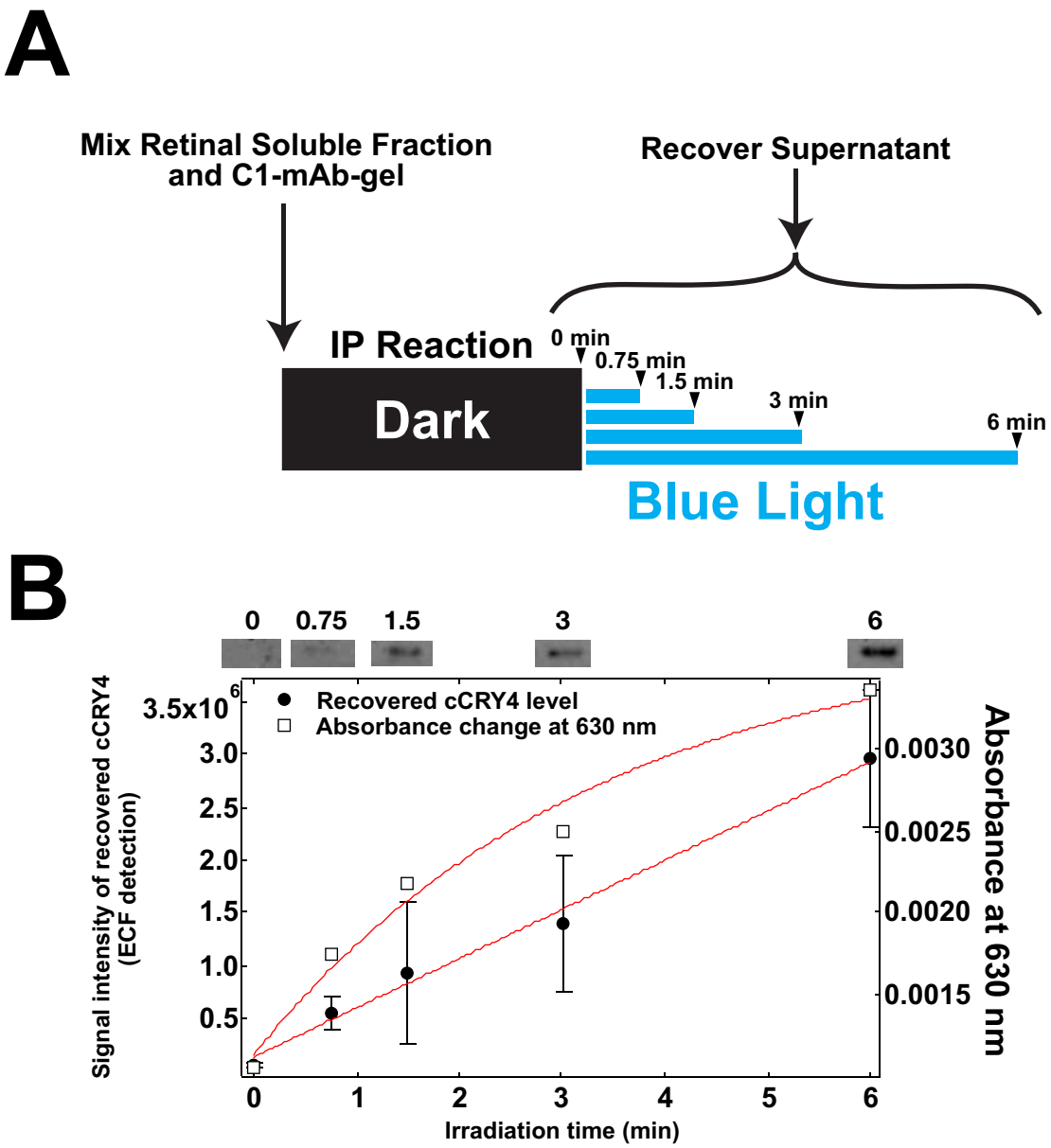
A
Mix Retinal Soluble Fraction and C1-mAb-gel
Recover Supernatant
IP Reaction
Dark
0 min
0.75 min
1.5 min
3 min
6 min
Blue Light
B
0
0.75
1.5
3
6
Recovered cCRY4 level
Absorbance change at 630 nm
3.5x10^6
3.0
2.5
2.0
1.5
1.0
0.5
Signal intensity of recovered cCRY4 (ECF detection)
0.0030
0.0025
0.0020
0.0015
Absorbance at 630 nm
0
1
2
3
4
5
6
Irradiation time (min)

Figure 7

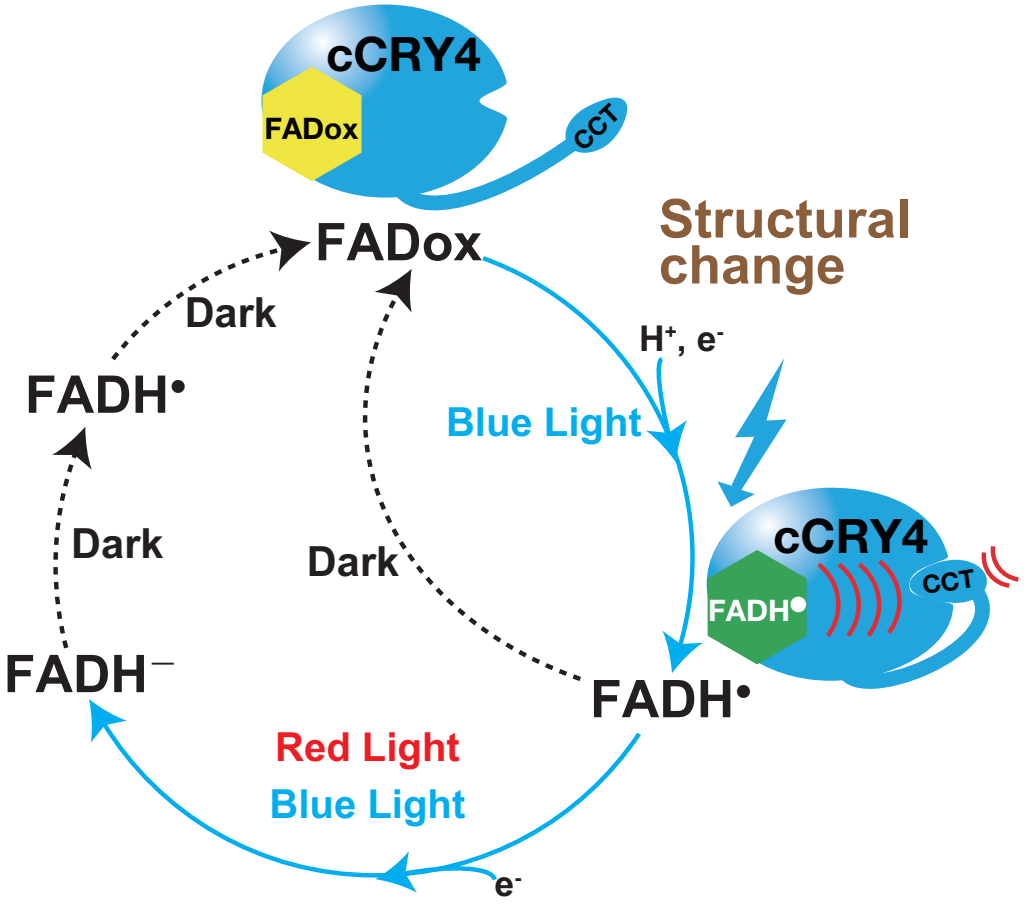
cCRY4
FADox
CCT
FADox
Structural change
H+, e-
Blue Light
Dark
FADH•
Dark
Dark
cCRY4
FADH•
CCT
FADH−
FADH•
Red Light
Blue Light
e-